JOURNAL OF MATERIALS SCIENCE 37 (2002) 4919–4927

Characterisation of the mechanical properties of plasma-polymerised coatings by nanoindentation and nanotribology

B. D. BEAKE*
Micro Materials Ltd., Unit 3, The Byre, Wrexham Technology Park, Wrexham, LL13 7YP, UK
E-mail: ben@micromaterials.co.uk
Web: www.micromaterials.co.uk

G. J. LEGGETT
Department of Chemistry, UMIST, Manchester, PO Box 88, M60 1QD, UK

M. R. ALEXANDER
Corrosion and Protection Centre, UMIST, Manchester, PO Box 88, M60 1QD, UK

Nanoindentation and SFM tip-induced wear (nanotribology) have shown clear differences in the mechanical properties of plasma-polymerised coatings when compared to conventional thermoplastics. Plasma polymers deposited in-plasma are much harder, stiffer and wear resistant than conventional polymers. Plasma polymers deposited downstream at low plasma power exhibit viscous behaviour. They are susceptible to nanowear and the resulting morphology of the worn region is completely different to what is observed on conventional polymers such as poly(ethylene terephthalate) and polystyrene.

1. Introduction

Plasma polymers are coatings that are normally prepared from non-equilibrium reduced pressure plasmas of gaseous and volatile organic compounds where synthesis and deposition occur simultaneously [1, 2]. Precise control over film thickness (1–100 nm) can be exercised and conformal pinhole-free film deposition can be achieved, even on substrates of complicated geometry. Polymerisation occurs without solvents in a reduced-pressure vessel which is self-contained thereby optimising waste management. Furthermore, deposits may be formed from compounds not amenable to conventional polymerisation, e.g., methane [3].

It is possible to produce organic and inorganic plasma deposits by choice of monomer, addition of gas, manipulation of plasma parameters and substrate temperature. Here, we will consider organic plasma polymers, although it should be noted that in some cases the myriad of chemical states formed by the plasma environment mean that a distinct boundary between polymeric and inorganic deposits does not always exist; see for example the deposition of silica-polydimethylsiloxane from hexamethyldisiloxane/oxygen plasma [4, 5].

Recently, there has been increased interest in synthesis of plasma polymer films with a high degree of chemical functionality retained from the monomer [6-8]. Retention of monomer functionality at the surface of a coating offers very high levels of control over interactions with the surface that are independent of the substrate chemistry, e.g., wetting and adhesion. This control can be further enhanced by copolymerisation, where a 'functionalised' monomer is polymerised with a 'diluent' hydrocarbon to achieve the desired concentration of a specific functionality [9]. This approach has been shown to provide control of both the concentration of the carboxylic acid functionality and the solubility of the deposits [10].

The many attractive and novel properties of plasma deposits have lead to the exploration of their application in a wide range of areas; including adhesion promotion [11, 12], corrosion protection of steel [13, 14] and archaeological objects .[3], blood contacting biomaterials [15–17], skin cell supports [18] membranes [19], conductive lightguides, [20] hydrophobic surfaces [21, 22] resists in microfabrication processes [23, 24] and diamond coatings [25].

In addition to performance-based assessment in these areas much successful characterisation of plasma polymers chemistry has been achieved using surface analysis techniques including contact angle, Fourier transform infra-red spectroscopy, x-ray photoelectron spectroscopy and secondary ion mass spectrometry. These surface specific techniques have proved very useful in the analysis of the very thin plasma deposits. Characterisation of the mechanical properties of these materials was carried out by residual stress measurements on flexible substrates [26] and scratch hardness measurements [27]. More recently the use of nanoindentation

*Author to whom all correspondence should be addressed.

[28] and nanotribological methods [29, 30] has been explored to provide information on the mechanical properties these materials. In this article we describe the preparation and characterisation of plasma polymerised hexane, focussing on the use of nanoindentation and scanning force microscopy (SFM) tip-induced wear (nanotribology) to assess their mechanical properties, and compare their behaviour to results on other bulk polymer films and thin coatings.

2. Preparation and characterisation of deposit chemistry

Plasma polymers are generally deposited from organic vapours and gases in reduced pressure systems, although it should be recognised that atmospheric pressure plasma systems are also under investigation in an attempt to reduce the capital cost of commercial systems [31]. High throughput commercial reduced pressure systems have been developed to semi-continuously coat web (1.5 m wide) [32], and the complex geometry of headlights for corrosion protection [33]. Thus far, reports of fully-continuous web coating are limited to e-beam physical vapour deposition (PVD) coating with prior plasma cleaning/activation of the aluminium surface [34].

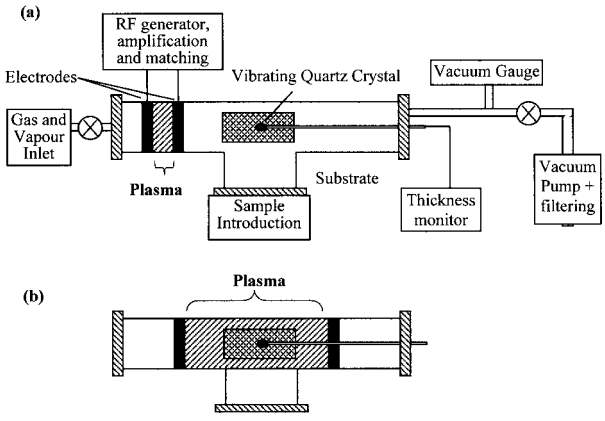

Figure 1 Schematic of the plasma deposition apparatus used with the substrate (opposite the quartz crystal) (a) downstream and (b) in the plasma.

A schematic of a typical laboratory scale deposition reactor is presented in Fig. 1. An estimate of the deposit thickness is obtained from a vibrating quartz crystal monitor positioned axisymetrically opposite to the sample that is supported on an aluminium plate. In this case external copper electrodes are used to capacitively couple the radio frequency (13.56 kHz) power supply to the plasma. To achieve in-plasma and downstream deposition the electrode configuration is altered, thus enabling the fixed Quartz Crystal Microbalance (QCMB) to be used for *in situ* thickness estimation.

This QCMB thickness estimate may be calibrated using a transmission electron microscopy (TEM) section of the type presented in Fig. 2 where a film of plasma polymerised hexane (ppHex) deposited on aluminium is shown. After an initiation period lasting about 25 seconds, deposition proceeded linearly with time.

X-ray photoelectron spectroscopy, using a Scienta ESCA300 instrument, of ppHex deposits has indicated that they have a low but significant oxygen component on an otherwise purely hydrocarbon structure as indicated from the C1s peak shape (Fig. 3). This is consistent with some incorporation of oxygen into the hydrocarbon surface, although the hydrophobic nature of the surface is indicated by the high water contact angles measured on such materials, i.e., 101°, measured using a KSV CAM200 instrument.

3. Nanoindentation

3.1. Introduction

The mechanical properties of bulk polymers have traditionally been evaluated by techniques such as microhardness and tensile testing which are not ideally suited to the investigation of thin films and coatings. Variations

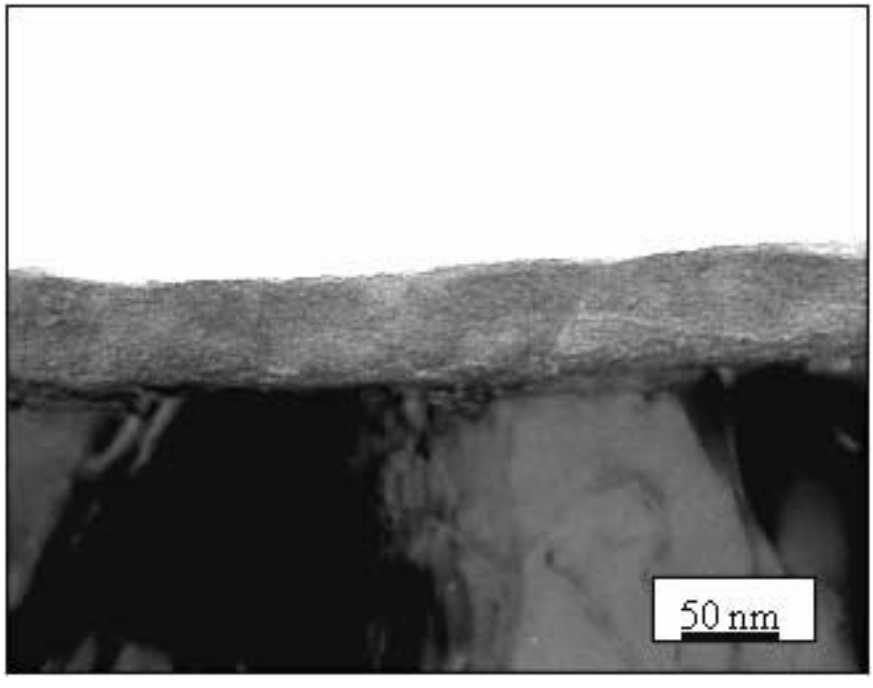

Figure 2 TEM section of a plasma polymerised hexane layer on aluminium (AA1050A).

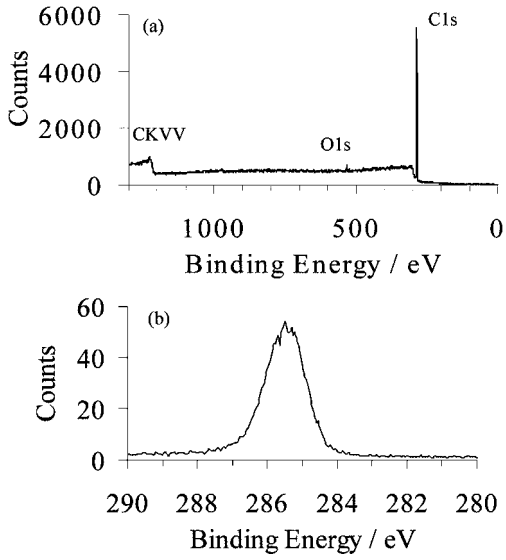

Figure 3 XPS widescan spectrum (a) and C1s core level (b) from plasma polymerised hexane on aluminium; [C] = 98% [O] = 2 at%. The spectra were acquired on a Scienta ESCA 300 spectrometer (RUSTI, Daresbury) no charge correction has been applied.

in microhardness have been correlated to known differences in crystallinity, molecular weight, cohesive energy density, microstructure, elastic modulus and yield stress [35–40]. Although this has provided valuable mechanical characterisation data for a wide range of bulk semicrystalline and amorphous polymers, it has limited usefulness for thin plasma polymerised coatings since the large applied loads and penetration depths necessary to image the resultant indent mean that the results are inevitably dominated by substrate contribution, and it does not provide information on their elastic properties.

Depth-sensing indentation techniques, which are capable of providing measurements of elastic and plastic properties at the sub-micron level can be used to optimise the mechanical properties of plasma-polymerised coatings. In depth-sensing indentation (or nanoindentation) the indentation process is continually monitored with respect to force, displacement and time.

With the exception of the contact area, the load-displacement curve (as shown in Fig. 4) contains all the values required for hardness and modulus determination. The contact depth, necessary to calculate contact area, is determined by fitting the upper 60–80% of the

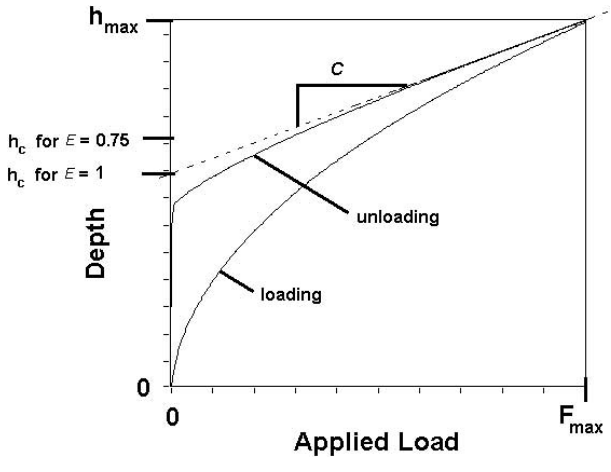

Figure 4 Force-displacement curve for a typical elastoplastic material.

unloading curve to a power law function, as originally proposed by Oliver and Pharr [41], of the form

$$F = a(h - h_f)^m \tag{1}$$

where F is the force, $(h - h_f)$ is the elastic displacement, and a and m are material constants. The contact depth, h_c, is determined from Sneddon's elastic analysis [42] using the expression

$$h_c = h_{\max} - \varepsilon(h_{\max} - h_f) \tag{2}$$

$$h_c = h_{\max} - \varepsilon(C F_{\max}) \tag{3}$$

where C is the contact compliance between the diamond indenter and the sample, equal to the tangent to the unloading curve at maximum load ($F_{\max}$) after correction for frame compliance.

Contact compliance C = total compliance (C_t)-frame compliance

$$(C_f) = \mathrm{d}h/\mathrm{d}F \tag{4}$$

The value of the geometric constant ε depends on the pressure distribution that is established after the plastic deformation which is a function of the indenter geometry. For a Berkovich indenter ε is usually taken as 0.75.

The hardness (H) is determined from the peak load $(F_{\max})$ and the projected (cross-sectional) area of contact, A_c, by:

$$H = \frac{F_{\max}}{A_c} \tag{5}$$

The reduced modulus, E_r, is defined as:

$$E_r = \frac{\sqrt{\pi}}{2.C}\frac{1}{\sqrt{A_C}} \tag{6}$$

$$\frac{1}{E_r} = \frac{1 - \nu_S^2}{E_S} + \frac{1 - \nu_i^2}{E_i} \tag{7}$$

where ν_s = Poisson's ratio for the sample, ν_i = Poisson's ratio for the diamond indenter (0.07), E_s = Young's modulus for the sample and E_i = Young's modulus for the indenter (1140 GPa). ν_s is close to 0.4 for many polymers.

Nanoindentation has been employed extensively to characterise the mechanical properties of a wide range of hard coatings and surface-engineered materials [43–49]. Recent studies such as the European project "Indicoat" have determined the conditions necessary for accurate hardness and modulus determination on hard and ductile coatings [50]. The measurement of the hardness of hard brittle coatings is only possible if the coating yields before the substrate. For very thin coatings the yield may be initiated in the substrate and the coating hardness value is never achieved, even with very sharp probes. The optimum test parameters for hardness and modulus measurement are slightly different; precise hardness determination requiring the use of sharp indenters whilst modulus measurement is aided by suppression of plastic effects e.g., by the use of spherical indenters. Results on ductile coatings were strongly influenced by creep when the holding period at maximum force was too short. It was noted that the apparent strain-rate sensitivity can be due to the absence of this hold

period in the loading-unloading cycle [50]. If the holding period at maximum force is absent or too short, the sample will continue to creep during unloading, distorting the shape of the unloading curve and leading to inaccurate values of the modulus, since it is determined from the tangent to the slope of the unloading curve at maximum load.

3.2. Bulk polymer films

For our studies of the nanomechanical properties of polymeric films and coatings a commercial nanoindentation instrument (NanoTest System manufactured by Micro Materials) has been used in load-controlled mode. Details of the specifications of the instrument have been published previously [51, 52]. The NanoTest is a pendulum-based depth-sensing system, with the sample mounted vertically and the load applied electromagnetically as shown schematically in Fig. 5. Current in the coil causes the pendulum to rotate on its frictionless pivot so that the diamond probe penetrates the sample surface. Test probe displacement is measured with a parallel plate capacitor with sub-nm resolution. The horizontal indentation configuration enables calibrated contact load to be applied and symmetrical indents to be produced.

Studies of the nanoindentation of polymers have been relatively rare [53–58], presumably due to the assumption that their time-dependent mechanical behaviour makes the interpretation of results problematic. However, several groups have shown that reliable measurements of the hardness and modulus on bulk polymers are possible. Beake and Leggett have investigated the effects of draw-induced orientation and crystallinity on the mechanical properties of poly(ethylene terephthalate) (PET) films [58]. Differences in their mechanical properties determined by nanoindentation correlated with differences in their resistance to microscale scratching wear. The optimum conditions for hardness and modulus measurement on PET were found to be a combination of a relatively slow loading rate together with a long holding period at maximum load to allow for creep. Flores and Baltá Calleja found similar optimum parameters in ultramicrohardness testing of amorphous PET films [56].

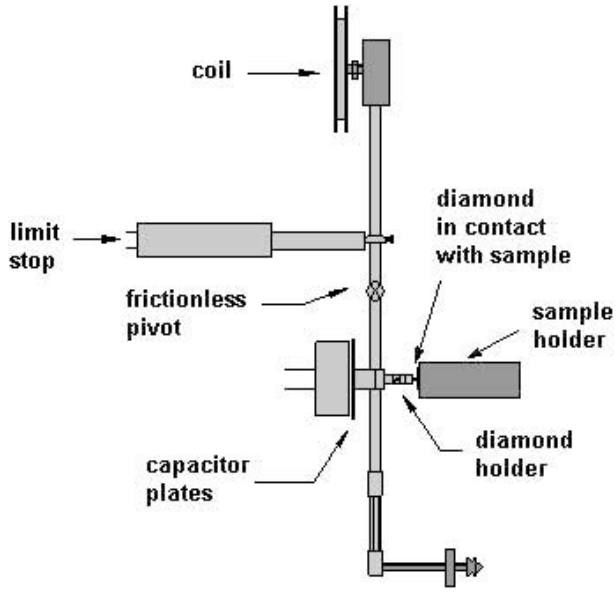

Figure 5 Schematic of the NanoTest system.

As the elastic and plastic properties are determined from the unloading curve, the loading curve data is usually considered of less importance although it often contains useful characterisation data. Inflexions in the loading slope can reveal substrate influence on the indentation behaviour of coatings (see Section 3.3 below) when indenting to an appreciable fraction of the coating thickness. Discrete pop-in effects can be due to phase transformations or to cracking that is related to the coating toughness [59].

Loading data can be fitted to a power-law function (Equation 7) to determine the loading exponent and depth offset:

$$F = a(h - h_0)^n \tag{7}$$

where F is the load, h_0 is the depth offset, a is a material parameter and n is the indentation exponent. Deviations from $n = 2$ can occur when (1) there is strain-rate hardening, (2) when there are viscoelastic effects, (3) when the indenter is not sharp and (4) where the mechanical properties vary with depth. For example, on poly(ethylene oxide) (PEO) films, the value of the loading exponent n varies strongly with synthesis method [60]. On solution-synthesised PEO films n was ~1.5, suggesting strongly viscoelastic behaviour and these materials showed strong strain-rate sensitivity and an indentation size effect in their hardness. In contrast, values of n for melt-synthesised PEO films were 1.8–1.9 (i.e., much closer to 2) implying less pronounced viscoelastic behaviour, and these materials showed minimal variation in hardness with indentation depth.

In addition to being necessary for the determination of accurate modulus measurements, the hold period at maximum load, and the indentation creep that occurs during it can be a useful additional characterisation tool in itself. Experimentally, it has been found that the variation of hardness with creep follows the form [51, 56]:

$$H = H_0 t^{-k} \tag{8}$$

where H_0 is the hardness measured at $t = 1$ min and k is the creep constant. Creep data acquired during the holding period at maximum load have been found to closely fit the general logarithmic equation for nanoindentation creep (Equation 9) [61].

$$h = A \ln(Bt + 1) \tag{9}$$

where $h =$ increase in depth, A and B are fitting parameters. The parameter A is a measure of the extent of creep and the parameter B is a measure of the rate of creep.

3.3. ppHex coatings

To obtain quantitative hardness and modulus data on ppHex coatings of thickness >200 nm we have used a similar approach to that taken on bulk polymers, i.e., a low loading rate (0.06 mN/s) together with a holding time at maximum load of at least 30 s. As mentioned above, for coating-only plastic response, it is important

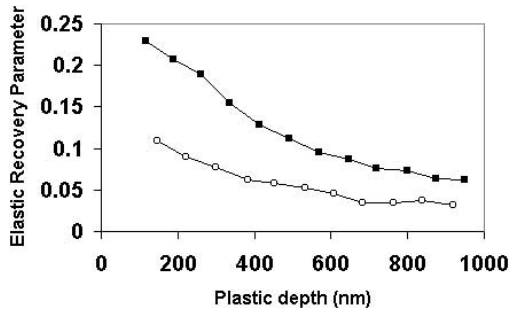

Figure 6 Variation in Elastic Recovery Parameter with plastic depth for 1500 nm thick 100 W (filled squares) and 25 W (open circles) ppHex coatings deposited in-plasma on Al.

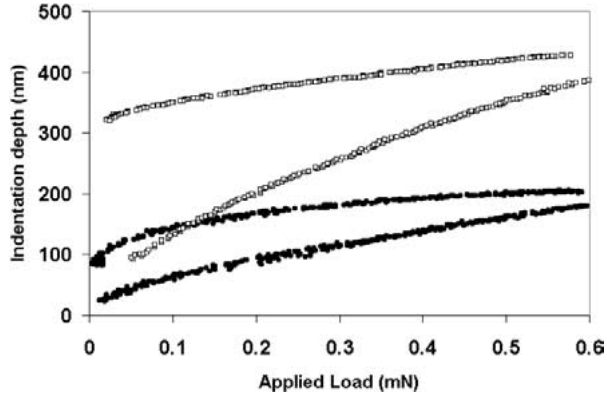

Figure 7 Indentation to 0.6 mN on uniaxially oriented PET film (open squares) and 25 W in-stream ppHex (filled circles).

that the stress field remains within the coating, and a rule of thumb that is often used is that the indentation depth should be less than one-tenth of the coating thickness for accurate hardness measurement. Indeed, for accurate modulus measurements even shallower indentations may be necessary [50]. At greater depths the influence of the substrate progressively dominates the mechanical response as shown in Fig. 6. The figure shows the variation in Elastic Recovery Parameter (ERP) with plastic depth determined from load-partial unload experiments. In this type of experiment several loading-unloading cycles to gradually increasing depth are performed allowing the variation in indentation response with depth to be investigated. The elastic recovery parameter is defined as:-

$$\text{Elastic recovery parameter} = (h_{\max} - h_p)/h_p \qquad (10)$$

where $h_{\max}$ = maximum depth and h_p = plastic (or contact) depth. The ERP is linearly related to the ratio of hardness to modulus (H/E) that defines the overall indentation behaviour and is a useful index as it is dimensionless and, for an ideally homogeneous sample, it is independent of depth or load [52]. In the figure the influence of substrate is seen even at shallow depths.

Table I shows the hardness and modulus determined from indentations to ∼1/10 coating thickness. The in-plasma ppHex coatings on Aluminium exhibit significantly greater hardness and modulus than conventional amorphous thermoplastics such as polystyrene [PS], poly(methylmethacrylate) [PMMA] and polycarbonate [PC], and semicrystalline materials such as PET and ultra-high molecular weight polyethylene [UHMWPE] [28, 54, 58, 62, 63]. Typical indentation curves on ppHex and PET are shown in Fig 7. Despite these differences the ppHex coatings have reasonably similar H/E ratio and hence elastic recovery during indentation. Increased hardness is often associated with greater susceptibility to brittle fracture and this has been observed for ppHex coatings in load-partial unload experiments. The hard and stiff in-plasma ppHex coatings are more resistant to indentation creep than most thermoplastics [28].

When the thickness of the plasma polymer coating is less than ∼200 nm it becomes difficult to use the above approach to obtain coating-only measurements of hardness and modulus. Quantitative measurement of the coating plastic properties requires (1) the stress field remains within the coating (2) the coating yields before the substrate. For very thin coatings yield may be initiated in the substrate and the coating hardness value is never achieved, even with very sharp probes [50].

Length-scale effects mean that it is not always possible to assume the properties of very thin coatings from measurements on thicker coatings. Several researchers have shown that a strong increase in ductility is observed in brittle polymers when the film thickness is reduced to the order of 30 nm [64–67]. Meijer and coworkers have used nanoindentation techniques to investigate amorphous PS sheet [68]. They used spherical indenters with different tip radii and compared computed and experimental behaviour on different length scales. To fit the experimental data for indentations to 100 nm it was necessary to modify their simulations to use lower yield stress and less strain softening with respect to bulk parameters to get good agreement, supporting the hypothesis that the observed length scale effect is due to a T_g effect near the free surface [68].

Although it is not always possible to directly measure the real coating hardness, it is possible to gain information for optimisation of the mechanical properties of thin polymer coatings by (1) using SFM nanotribology as described in the next section and (2) using nanoindentation to obtain other mechanical property information such as modulus, creep and adhesion.

Using larger radius probes suppresses the onset of plasticity and brittle failure and so can be employed to measure the coating modulus, as recommended for the study of engineering coatings [50]. The coating modulus is obtained by extrapolating the modulus vs. depth to zero depth.

When sharper probes are used for coating-only plastic response, the stress field should remain within the coating; deeper indentations can show inflections

TABLE I Mechanical properties of plasma polymerised ppHex coatings deposited in-plasma on Al

Material	Hardness (GPa)	Reduced modulus (GPa)	Elastic recovery parameter
100 W	0.68	10.0	0.26
25 W	0.48	13.5	0.14
Biaxial PET[a]	0.29	4.4	0.24
Uniaxial PET[a]	0.14	3.4	0.14

[a]From indentations to 0.5 mN.

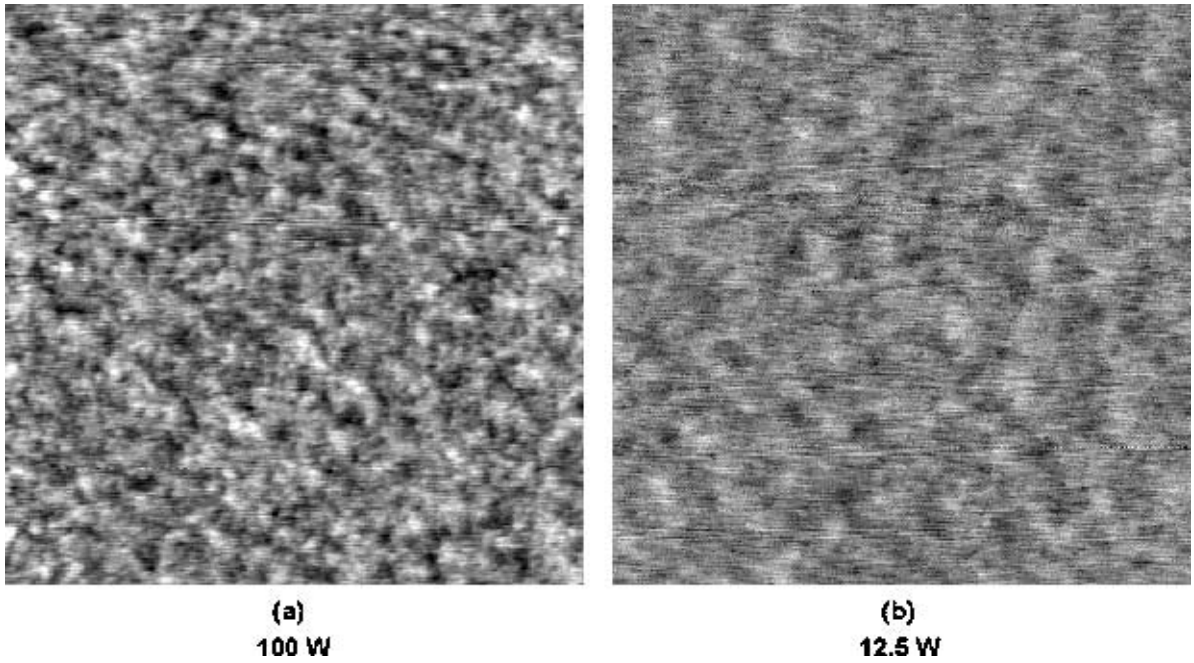

Figure 8 $1 \times 1\,\mu$m Tapping mode images of (a) 100 W downstream ppHex coating on mica and (b) 12.5 W downstream ppHex coating on mica. Z-scale 5 nm. Tapping conditions: Si cantilever driven at resonance (280.5 kHz), free-amplitude of oscillation 13–15 nm, ratio of set point to amplitude of oscillation 0.9, 1 Hz scan frequency.

reflecting the transition into substrate and these can be used to determine whether the coating is harder than the substrate. Benítez and co-workers have investigated the nanoindentation behaviour of 220 nm thick films of thin films of plasma polymerised hexamethyl disiloxane in a DC glow discharge plasma [69–71] deposited on polycarbonate (PC) substrate. They observed a clear and reproducible inflexion in the slope of the force-displacement curve at ∼80 nm depth. This behaviour is typical of the transfer of load support from a harder coating to a softer substrate or sub-layer as the stress field penetrates further into the material with increasing force.

Sharp probes also can lead to discrete pop-in events during loading due to cracking and fracture. These are commonly seen on thin ppHex coatings. Similarly, den Toonder and co-workers have recently used nanoindentation to induce cracks together with *in situ* optical examination of fracture surfaces to determine the fracture toughness and adhesion energy of particle filled sol-gel coatings (methyltrimethoxysilane filled with silica nano-particles) on glass [59].

4. Nanotribology

4.1. Introduction

Scanning force microscopy [SFM] was originally developed primarily as a tool to obtain detailed images of surface topography and atomic structure. To obtain wear-free images of the topography of ppHex surfaces it is necessary to use tapping mode SFM (Fig. 8) where the intermittent contact forces and shear forces are lower than in contact mode [29]. In contact mode the local interfacial behaviour (adhesion and friction) can be studied. Modification of the SFM probe tip chemistry gives indirect chemical sensitivity. For example, with a hydrophilic tip coating the measured friction and adhesion forces in air vary with the proportion of oxygen-containing functionalities on the sample surface [72–74]. With contact forces of ∼5–50 nN contact mode SFM (which has been coined "wear mode" [29]) easily damages the surfaces of polymer coatings and can be used to study the nanotribology of thin polymeric coatings.

For experiments on polymers it is necessary to use a tip-cantilever assembly of lower force constant than is employed in nanoindentation so that the load applied can be in the nN range. The extent of deformation is too great when higher (μN) forces are used; the deformed material tends to attach to the tip and is dragged across the scan area during making accurate imaging impossible.

4.2. Nanowear of thermoplastics and ppHex

Conventional thermoplastics are easily deformed by the scanning of a SFM tip at very low contact forces [75–91]. The typical wear morphology of alternating ridges and troughs perpendicular to the fast scan axis has been interpreted as a stick-slip process. In contrast, our studies of the nanotribological behaviour of ppHex coatings reveal a very different wear morphology. This is illustrated for a ppHex coating deposited downstream of the plasma at low power in Fig. 9. The line profiles show schematically the development of the wear morphology with continued scanning for the two types of surface. On the plasma polymer appreciable viscous yield is seen at the turning points where the tip stops and inverts its scan direction resulting in deep grooves at the edge of the scan area. On both materials, although the worn region is much rougher after scanning its average depth relative to the surrounding surface remains unchanged.

The SFM experiments also show clear differences in nanowear between ppHex coatings on mica deposited

TABLE II Roughness of $2 \times 2\,\mu$m areas after scanning plasma-polymerised hexane film deposited on mica downstream of the plasma at 12.5 W for 3 scans at applied load of 6.4 nN

Scan rate (Hz)	Number of scan lines	Roughness (nm)
2	512	6.2
11	512	3.0
11	256	1.4
11	128	0.5

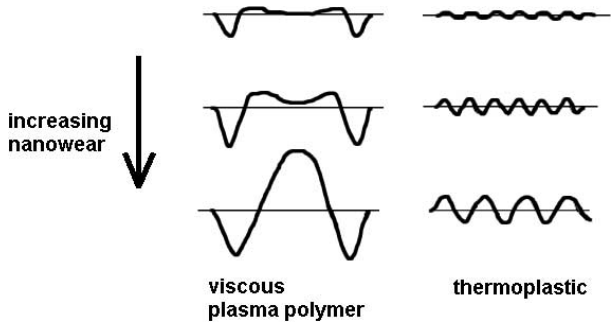

Figure 9 Schematic representation of the development of the nanowear morphology on (a) plasma polymer deposited downstream of the plasma at low power and (b) conventional thermoplastic (PET).

in-plasma and downstream of it. When deposited downstream of the plasma, coatings deposited at low power show viscous yield. The extent of wear is strongly dependent on the scanning parameters such as the number of scan lines (sampling density) and the scan speed as illustrated in Table II. As the scan speed is reduced the sample roughness increases significantly.

When deposited at higher plasma power the coatings are very resistant to nanowear, even when deposited downstream of the plasma. This suggests that changing the deposition power can produce coatings with widely differing yield strength at the nanoscale, and hence coatings deposited at higher power do not wear at the contact pressures in the SFM experiment. With repeat scanning of coatings deposited at high powers a slow fatigue process occurs and some deformation is observed.

Dinelli and co-workers have shown [30] that the extent of nanowear on in-plasma ppHex coatings on mica does not vary with scanning speed, and that films at low power are resistant to tip-induced wear, as might be expected from the high hardness and modulus determined from the nanoindentation testing of coatings on Al. They noted that the wear-resistance of in-plasma coatings increased with time, which was interpreted in terms of increased plasma-surface interactions leading to greater radical formation with exposure time and hence more cross-linking [30]. For a given deposition power, coatings deposited downstream of the plasma do not have the same interaction with the plasma and so are less cross-linked and hence more viscous.

4.3. Parameters to define nanowear

The nanowear experiment is well-defined: wear is by a single-asperity and hence the contact pressure under the probe is known accurately. However, Fig. 9 shows that conventional concepts for defining the wear resistance, such as wear depth or wear volume are not easily transferable to the nanoscale, since, as Fig. 9 shows, the average depth of the worn region is the same after wear as before. This is because the primary deformation processes involve plastic deformation and viscous yield; extensive breaking of C─C bonds and the movement of material from the wear region does not occur until greater loads are applied.

TABLE III Nanoscale wear regimes of plasma polymers and thermoplastics

Material	Crystallinity/ microstructure	Nanowear deformation process	Ref.
PpHex deposited at low power[a]	Lightly cross-linked network	Viscous yield	29
Low MW PS	Amorphous	Viscous yield	75
High MW PS	Amorphous	Plastic deformation	75
Uniaxial PET	30% crystallinity	Plastic deformation	77
Biaxial PET	50% crystallinity	Fatigue	76
PpHex deposited at high power[a]	Highly cross-linked network	Fatigue	29

[a]Deposited downstream of the plasma on mica.

It is necessary to use other parameters to define the extent of nanoscale wear. Fig. 9 and Table III show that the observed wear morphology is a sensible choice. Results show that the observed wear morphology is a strong function of entanglement density on amorphous polymers, crystallinity on semicrystalline thermoplastics and cross-link density on plasma polymers [29, 30, 75–77]. How this observed wear morphology develops with continued scanning and its sensitivity to the experimental parameters both provide useful information on the nature of the deformation process. Experimentally, the surface roughness increases with the extent of deformation, so a measure of surface roughness such as R_a, or R.M.S. roughness is a useful semi-quantitative parameter. The change in sample roughness (or rate of change of roughness) with continued scanning can describe the fatigue process.

Dinelli and co-workers have shown that it is possible to also use the "critical load" for deformation as a measure of the nanowear resistance of ppHex coatings [30]. An area is imaged at a given force and re-scanned at lower force and lower magnification to observe whether there is any difference between the previously scanned area and the surrounding surface. It has been successfully used to show differences with deposition power, number of scan cycles and in-plasma/downstream. The idea is similar to the multi-pass scratch testing technique developed at the micro-scale [92], where number of cycles to failure at constant load is used as a measure of coating adhesion, and indeed, delamination of ppHex coatings can occur after a few scan cycles even at very low contact loads in the SFM experiment.

5. Concluding remarks

The results described in this paper illustrate the very significant differences in mechanical properties of ppHex plasma polymers when compared with conventional polymer materials revealed by both nanotribology and nanoindentation. Plasma polymers deposited in-plasma are much harder, stiffer and wear resistant than conventional polymers. Plasma polymers deposited

downstream at low power exhibit viscous behaviour. They are susceptible to nanowear and the resulting morphology of the worn region is different to that on conventional polymers such as PET and PS. The very clear differences with sample location (in-plasma or downstream of the plasma) deposition power and deposition time revealed by the nanoscale testing techniques show that they are very useful tools in the optimisation of the mechanical properties of thin coatings. The approach described is also finding success in characterising the mechanical properties of other polymer coatings and thin films.

Acknowledgements

MRA thanks the EPSRC for the award of an Advanced Research Fellowship (AF/98/0740) and access to the RUSTI ESCA300 instrument at Daresbury Laboratory.

References

1. H. YASUDA, in "Plasma Polymerisation" (Academic Press, New York, 1985).
2. R. D'AGOSTINO, in "Plasma Deposition, Treatment, and Etching of Polymers" (London: Academic Press, 1990).
3. L. FAVRE-QUATTROPANI, P. GROENING, D. RAMSEYER and L. SCHLAPBACH, *Surf. Coat. Tech.* **125** (2000) 377.
4. M. R. ALEXANDER, R. D. SHORT, F. R. JONES, W. MICHAELI and C. J. BLOMFIELD, *Appl. Surf. Sci.* **137** (1999) 179.
5. M. R. ALEXANDER, R. D. SHORT, F. R. JONES, M. STOLLENWERK, J. ZABOLD and W. MICHAELI, *J. Mater. Sci.* **31** (1996) 1879.
6. L. O'TOOLE, A. J. BECK and R. D. SHORT, *Macromolecules* **29** (1996) 5172.
7. C. L. RINSCH, X. L. CHEN, V. PANCHALINGAM, R. C. EBERHART, J. H. WANG and R. B. TIMMONS, *Langmuir* **12** (1996) 2995.
8. C. I. BUTOI, N. M. MACKIE, L. J. GAMBLE, D. G. CASTNER, J. BARND, A. M. MILLER and E. R. FISHER, *Chem. Mater.* **12** (2000) 2014.
9. A. J. BECK, F. R. JONES and R. D. SHORT, *Polymer* **37** (1996) 5537.
10. M. R. ALEXANDER and T. M. DUC, *ibid.* **40** (1999) 5479.
11. A. P. KETTLE, F. R. JONES, M. R. ALEXANDER, R. D. SHORT, M. STOLLENWERK, J. ZABOLD, W. MICHAELI, W. WU, E. JACOBS and I. VERPOEST, *Composites Part A-Appl. Sci. Manufact.* **29** (1998) 241.
12. M. R. ALEXANDER, X. ZHOU, G. E. THOMPSON, T. M. DUC, E. MCALPINE and B. J. TIELSCH, *Surf. Interface Anal.* **30** (2000) 16.
13. Y. TSAI and F. BOERIO, *J. Appl. Polym. Sci.* **10** (1998) 1283.
14. T. LIN, J. ANTONELLI, D. YANG, H. YASUDA and F. WANG, *Prog. Org. Coat.* **31** (1997) 351.
15. T.-M. KO and S. COOPER, *J. Appl. Polym. Sci.* **47** (1993) 1601.
16. J. M. GRUNKEMEIER, W. B. TSAI, M. R. ALEXANDER, D. G. CASTNER and T. A. HORBETT, *J. Biomed. Mater. Res.* **51** (2000) 669.
17. M. C. SHEN, Y. V. PAN, M. S. WAGNER, K. D. HAUCH, D. G. CASTNER, B. D. RATNER and T. A. HORBETT, *J. Biomater. Sci.-Polym. Ed.* **12** (2001) 961.
18. D. B. HADDOW, R. M. FRANCE, R. D. SHORT, S. MACNEIL, R. A. DAWSON, G. J. LEGGETT and E. COOPER, *J. Biomed. Mater. Res.* **47** (1999) 379.
19. A. HOLLAHAN and T. WYDEVEN, *Science* **179** (1973) 500.
20. G. SMOLINSKY, P. TIEN and M. VASILE, US Patent no. 3,822,928 (1974).
21. A. J. GRIGGS, V. LEY and R. B. TIMMONS, *Abstr. Pap. Am. Chem. Soc.* **221** (2001) 708.
22. S. COULSON, I. WOODWARD, J. BADYAL, S. BREWER and C. WILLIS, *Chem. Mater.* **12** (2000) 2031.
23. S. HATTORI, M. YAMADA, J. TAMANO, M. IEDA, S. MORITA, K. YONEDA and S. IDEDA, *J. Appl. Polym. Sci. Appl. Polym. Sym.* **38** (1984) 127.
24. L. SHEPSIS, P. PEDROW, R. MAHALINGAM and M. OSMAN, *Thin Solid Films* **11** (2001) 385.
25. K. KURIHARA, K. SASAKI, M. KAWARADA and N. KOSHINO, *Appl. Phys. Lett.* **52** (1988) 437.
26. A. MORINAKA and Y. ASANO, *J. Appl. Polym. Sci. Appl. Polym. Sym.* **27** (1982) 2139.
27. K. CHEN, N. INAGAKI and K. KATSUURA, *J. Appl. Poly. Sci.* **27** (1982).
28. B. D. BEAKE, S. ZHENG and M. R. ALEXANDER, *J. Mater. Sci.*, in press.
29. B. D. BEAKE, G. J. LEGGETT and M. R. ALEXANDER, *Polymer* **42** (2001) 2647.
30. F. DINELLI, G. J. LEGGETT and M. R. ALEXANDER, *J. Appl. Phys.* **91** (2002) 3841.
31. S. E. BABAYAN, J. Y. JEONG, A. SCHUTZE, V. J. TU, M. MORAVEJ, G. S. SELWYN and R. F. HICKS, *Plasma Sources Sci. Tech.* **10** (2001) 573.
32. M. CREATORE, F. PALUMBO, R. D'AGOSTINO and P. FAYET, *Surf. Coat. Tech.* **142–144** (2001) 163.
33. H. GRÜNWALD, R. ADAM, J. BARTELLA, M. JUNG, W. DICKEN, S. KUNKEL, K. NAUENBURG, T. GEBELE, S. MITZLAFF, G. ICKES, U. PATZA and J. SNYDERB, *Surf. Coat. Tech.* **111** (1999) 287.
34. E. REINHOLD, J. RICHTER, H. WAYDBRINK and E. ZSCHIESCHANG, *Thin Solid Films* **377** (2000) 14.
35. S. FAKIROV, F. J. BALTÁ CALLEJA and M. KRUMOVA, *J. Polym. Sci. Polym. Phys. Ed.* **37** (1999) 1413.
36. M. KRUMOVA, S. FAKIROV, F.J. BALTÁ CALLEJA and M. EVSTATIEV, *J. Mater. Sci.* **33** (1998) 2857.
37. C. VANDEROCKT, M. KRUMOVA, F. J. BALTÁ CALLEJA, H. G. ZACHMANN and S. FAKIROV, *Colloid Polym. Sci.* **276** (1998) 138.
38. J. MARTÍNEZ-SALAZAR, J. GARCÍA PEÑA and F. J. BALTÁ CALLEJA, *Poly. Commun.* **26** (1985) 57.
39. C. SANTA CRUZ, F. J. BALTÁ CALLEJA, H. G. ZACHMANN, N. STIBECK and T. ASANO, *J. Polym. Sci.* B **29** (1991) 819.
40. C. SANTA CRUZ, F. J. BALTÁ CALLEJA, T. ASANO and I. M. WARD, *Phil. Mag.* (1993) 68.
41. W. C. OLIVER and G. M. PHARR, *J. Mat. Res.* **7** (1992) 1564.
42. I. D. SNEDDON, *Int. J. Eng. Sci.* **3** (1965) 47.
43. E. MARTÍNEZ, M. C. POLO, E. PASCUAL and J. ESTEVE, *Diam. Relat. Mater.* **8** (1999) 563.
44. A. LOUSA, E. MARTÍNEZ, J. ESTEVE and E. PASCUAL, *Thin Solid Films* **355/356** (1999) 210.
45. J. ESTEVE, E. MARTÍNEZ, A. LOUSA, F. MONTALÀ and L. L. CARRERAS, *Surf. Coat. Tech.* **133/134** (2000) 314.
46. J. L. MENEVE, J. F. SMITH, N. M. JENNETT and S. R. SAUNDERS, *Appl. Surf. Sci.* **100/101** (1996) 64.
47. M. F. DOERNER and W. D. NIX, *J. Mat. Res.* **1** (1986) 601.
48. R. DEKEMPENEER, R. JACOBS, J. SMEETS, J. MENEVE, L. ERSELS, B. BLANPAIN, J. ROOS and D. J. OSTRA, *Thin Solid Films* **217** (1992) 56.
49. N. M. JENNETT and A. J. BUSHBY, in press.
50. INDICOAT Final Report, NPL Report MATC(A) 24, NPL, Teddington, UK (2001).
51. F. J. BALTÁ CALLEJA and S. FAKIROV in "Microhardness of Polymers" (Cambridge University Press, Cambridge UK, 2000).
52. H. M. POLLOCK, "Nanoindentation," ASM Handbook, Vol. **18** (1992) p. 419.
53. R. H. ION, H. M. POLLOCK and C. ROQUES-CARMES, *J. Mater. Sci.* **25** (1990) 1444.
54. B. J. BRISCOE, L. FIORI and E. PELILLO, *J. Phys.* D **31** (1998) 2395.
55. R. S. DWYER-JOYCE, Y. USHIJIMA, Y. MURAKAMI and R. SHIBUTA, *Tribol. Int.* **31** (1998) 525.
56. A. FLORES and F. J. BALTÁ CALLEJA, *Phil. Mag.* A **78** (1998) 1283.
57. M. R. VANLANDINGHAM, J. S. VILLARRUBIA, W. F. GUTHRIE and G. F. MEYERS, *Macromol. Symp.* **167** (2001) 15.

58. B. D. BEAKE and G. J. LEGGETT, *Polymer* **43** (2002) 319.
59. J. M. J. DEN TOONDER, J. MALZBENDER, R. BALKENENDE and G. DE WITH, 2nd International Indentation Workshop, Cambridge, UK, July 2001.
60. B. D. BEAKE, S. CHEN, J. B. HULL and F. GAO, *J. Nanosci. Nanotech.* **2** (2002) 73.
61. T. CHUDOBA and F. RICHTER, *Surf. Coat. Tech.* **148** (2001) 191.
62. H. DONG and T. BELL *et al*., First Annual Project Report, Inco-Copernicus IC15-CT96-0705 (1998).
63. H. DONG and T. BELL, *Surf. Coat. Tech.* **111** (1999) 29.
64. A. J. L. MAGALHAES and R. J. M. BORGGREVE, *Macromolecules* **28** (1995) 5841.
65. M. C. M. VAN DER SANDEN, H. E. H. MEIJER and P. J. LEMSTRA, *Polymer* **34** (1993) 2148.
66. J. A. FORREST, K. DALNOKI-VERESS, J. R. STEVENS and J. R. DULCHER, *Phys. Rev. Lett.* **77** (1996) 2002.
67. J. L. KEDDIE, R. A. L. JONES and R. A. CORY, *Europhys. Lett.* **27** (1994) 59.
68. H. VAN MELICK, A. VAN DIJKEN, J. M. J. DEN TOONDER, L. GOVAERT and H. MEIJER, 2nd International Indentation Workshop, Cambridge, UK, July 2001 and *Phil. Mag.* A **82** (2002) 2093.
69. F. BENÍTEZ, E. MARTÍNEZ, M. GALÁN, J. SERRAT and J. ESTEVE, *Surf. Coat. Tech.* **125** (2000) 383.
70. J. ESTEVE, F. BENÍTEZ, S. BOSCH, E. MARTÍNEZ, M. GALÁN and J. SERRAT, Proc. SPIE 2000, San Diego.
71. F. BENÍTEZ, E. MARTÍNEZ and J. ESTEVE, *Thin Solid Films* **377/378** (2000) 109.
72. B. D. BEAKE and G. J. LEGGETT, *Phys. Chem. Chem. Phys.* **1** (1999) 3345.
73. B. D. BEAKE and G. J. LEGGETT, *Langmuir* **16** (2000) 735.
74. B. D. BEAKE, J. S. G. LING and G. J. LEGGETT, *J. Mater. Chem.* **8** (1998) 2845.
75. F. DINELLI, P. H. SHIPWAY and G. J. LEGGETT, *J. Appl. Phys.* **91** (2002) 3841.
76. B. D. BEAKE, G. J. LEGGETT and P. H. SHIPWAY, *Polymer* **42** (2001) 7025.
77. B. D. BEAKE, P. H. SHIPWAY and G. J. LEGGETT, in preparation.
78. J. S. G. LING, G. J. LEGGETT and A. J. MURRAY, *Polymer* **39** (1998) 5913.
79. S. A. C. GOULD, D. A. SCHIRALDI and M. L. J. OCCELI, *Appl. Poly. Sci.* **65** (1997) 1237.
80. R. JING, P. N. HENRIKSEN, H. WANG and P. J. MARTENY, *J. Mater. Sci.* **30** (1995) 5700.
81. S. N. MAGANOV and D. H. RENEKER, *Annu. Rev. Mater. Sci.* **25** (1997) 175.
82. V. V. TSUKRUK, *Rubber Chem. Tech.* **70** (1997) 430.
83. R. W. CARPICK and M. SALMERON, *Chem. Rev.* **97** (1997) 1163.
84. X. JIN and W. N. UNERTL, *Appl. Phys. Lett.* **61** (1992) 657.
85. O. M. LEUNG and M. C. GOH, *Science* **255** (1992) 64.
86. G. F. MEYERS, B. M. DEKOVEN and J. T. SEITZ, *Langmuir* **8** (1992) 2230.
87. G. J. VANCSO, T. D. ALLSTON, I. CHUN, L. S. JOHNANSSON, G. LIU and P. F. SMITH, *J. Polym. Anal. Char.* **3** (1996) 89.
88. D. D. WOODLAND and W. N. UNERTL, *Wear* **203/204** (1997) 685.
89. A. GANNEPALI, M. D. PORTER and S. K. MALLAPARAGADA, *Abstr. Pap. Am. Chem. Soc.* **215** (1998) NO. PT2, 002-PMSE.
90. Z. ELKAAKOUR, J. P. AIMÉ, T. BOUCHACINA, C. ODIN and T. MASUDA, *Phys. Rev. Lett.* **73** (1994) 3231.
91. A. KHURSHUDOV and K. KATO, *Wear* **205** (1997) 1.
92. MMST (EU-funded project SMT4972150).

Received 27 March
and accepted 8 June 2002